JOURNAL OF CATALYSIS 134, 75–86 (1992)

Vanadia, Vanadia–Titania, and Vanadia–Titania–Silica Gels: Structural Genesis and Catalytic Behavior in the Reduction of Nitric Oxide with Ammonia

BRENT E. HANDY, MAREK MACIEJEWSKI,[1] AND ALFONS BAIKER[2]

Department of Chemical Engineering and Industrial Chemistry, Swiss Federal Institute of Technology, ETH-Zentrum, CH-8092 Zürich, Switzerland

Received May 2, 1991

Metal oxide xerogels of pure vanadia, vanadia–titania, and vanadia–titania–silica were prepared by the hydrolysis of vanadium, titanium, and silicon alkoxides. The structural and chemical transformations of the gels occurring during thermal treatment under oxidizing and inert gas atmosphere were studied using thermoanalytical methods (TG, DTA) combined with mass spectroscopy, X-ray diffraction, and electron microscopy. Crystallization of the amorphous vanadia was found to be considerably retarded in the mixed gels compared to the pure vanadia gel. The mixed gels remain amorphous at 520 K, whereas crystallization already occurs in the pure vanadia gel at this temperature. All mixed gel phases separate after stabilization at 870 K, with the formation of V_2O_5 platelets and globular TiO_2 (anatase) particles. No other phases were detected by X-ray diffraction at this temperature. Addition of silica sol increases the overall surface area of the gel catalysts. This, however, does not increase the dispersion of vanadia in the amorphous matrix or stabilize it sufficiently to prevent crystallization under oxidizing conditions. Heat treatment of the gels at temperatures close to the melting point of vanadia results in rapid transformation of anatase to rutile. The stability and catalytic activity of the gels for the selective catalytic reduction of NO with NH_3 (SCR) were studied following thermal treatments under *in situ* and oxidizing (7% O_2) atmosphere. Low temperature SCR testing ($T \leq 520$ K) showed that the same kinetic behavior typical of titania-supported vanadia exists in all gels, with activity behavior being a function of gel composition and dispersion.

INTRODUCTION

Vanadia-based catalysts are highly active and selective for the selective catalytic reduction (SCR) of NO with NH_3, yielding almost exclusively nitrogen product for temperatures below 600 K (*1*). At issue in these catalysts is the active phase structure, reducibility, and dispersion of vanadia, which can be influenced by support type, and preparation conditions. Low-loaded, well-dispersed vanadia catalysts (*2*) often perform as well as co-precipitated catalysts (*3*), yet may contain considerably less vanadia as in the latter catalyst. One way of synthesizing well-dispersed and "molecularly-mixed" components of defined pore structure and crystallinity is by the sol–gel method (*4–7*), using metal alkoxides as precursor molecules. Since the precursors and solvents used may be obtained in high purity, the purity and compositional homogeneity of dried gels and ceramics may be more precisely controlled than in other methods. As-prepared V_2O_5–TiO_2 catalysts, with V_2O_5 contents up to 10%, showed large improvements in NO conversion with increasing vanadia content (*8*), with the catalyst containing 10% V_2O_5 of activity comparable to conventionally prepared catalyst, although catalyst activity declined due to surface area loss from anatase to rutile conversion of the TiO_2.

Mixed gels from hydrolyzed vanadium and silicon alkoxides were more thermally stable, having been calcined at 870 K prior

[1] On leave from Department of Chemistry, Warsaw University of Technology, Poland.

[2] To whom correspondence should be addressed.

0021-9517/92 $3.00

to catalytic use (*9*). These gels were amorphous for concentrations less than 10% V_2O_5, but microcrystalline domains of partially reduced vanadia phases were detected at higher loadings. Highest specific activities, in terms of mols NO converted per V^{5+} basis, estimated from TPR, were registered for the 1 and 10% V_2O_5 catalysts. Activity loss was also noted at higher temperatures for catalysts containing higher V_2O_5 contents; however, the unstable nature that was seen in V_2O_5–SiO_2 catalysts prepared by a grafting method (*10*) is absent from any of the mixed gel catalysts. Structural transformation of the amorphous gel is often dependent upon the treatment conditions. With pure vanadia gel activated at 520 K under *in situ* conditions for methanol oxidation to formaldehyde, catalytic activity increased with time on stream, achieving a steady state level nearly 30 times higher than the initial level (*11*). This was due to the crystallization of partially reduced vanadia phases in the gel, which is not seen with catalysts initially consisting of V_2O_5 crystallites.

Here we compare the reaction behavior and structural evolution of vanadia in a pure gel and in a mixed oxide gel matrix. The structural and catalytic properties of SCR of pure vanadia gel are contrasted with the corresponding properties of mixed vanadia–titania gel of 1 : 1 V : Ti mole ratio, and a ternary gel mixture formed by combining the sol of mixed vanadia–titania with an amount of pure silica sol to give a V : Ti : Si mole ratio of 1 : 1 : 2.

EXPERIMENTAL

Catalyst Preparation

All gels were made from the hydrolysis of vanadyl triisopropoxide (VTIP; Alfa Products, Inc., ca. 98%), titanium tetraisopropoxide (TIOT; Fluka Chemicals, Inc., ≥95%), and silicon tetraethoxide (TEOS; Fluka Chemicals, Inc., ≥98%). All metal alkoxides were used without further purification. All hydrolysis–gelation steps were performed at ambient temperature. To form the porous xerogels, excess solvent was removed by first drying on a Büchi rotating evaporator at 320–350 K, followed by drying overnight in a muffle oven maintained at 393 K.

Pure vanadia gel (V Gel) was formed by the slow addition of pH = 9 ammonia water (diluted 4 : 1 in isopropanol) to VTIP (diluted 5 : 1 in isopropanol) to a water-to-VTIP ratio of 10/1. A thick reddish-orange wet gel was formed, which upon drying turned dark green.

The binary vanadia–titania gel (VTi Gel) of V : Ti = 1 : 1 content was formed by first adding enough distilled water (diluted 5 : 1 with isopropanol) to TIOT (diluted 4 : 1 in isopropanol) until a water-to-TIOT ratio of two was reached, or theoretically, half the stoichiometric amount of water to displace fully the isopropoxy groups on TIOT. An appropriate amount of VTIP (diluted 4 : 1 in isopropanol) was then added to achieve the 1 : 1 V : Ti ratio. After stirring the mixed sol for ca. 30 min, hydrolysis was completed by an excess addition of distilled water (diluted 4 : 1 in isopropanol). The wet gel was orange-colored and upon solvent removal became a yellow-green xerogel.

The ternary gel of 1 : 1 : 2 V : Ti : Si mole proportions (VTiSi Gel) was formed in the following way. A silica gel was prepared by vigorously stirring a 2 : 1 (v/v) distilled water : TEOS mixture for ca. 20 h at ambient temperature. The white translucent sol was then added to an appropriate portion of the wet orange gel of the VTi Gel, and stirred for several hours to insure a homogeneous gel mixture. The mixture dried to a dark green, brittle xerogel.

Catalyst Characterization

Structural transformation of gels. Thermoanalytical studies (differential thermal analysis, DTA; and thermogravimetry, TG) were performed on a Netzsch STA 409, using a sample size of 20–50 mg and a heating rate of 10 K/min. Runs were performed in both flowing argon (60 cm^3min^{-1}) and in flowing air (60 cm^3min^{-1}). Gases evolved

during runs could be monitored with a Balzers QMG 424 mass spectrometer. X-ray powder diffraction patterns of the gels were measured on a Siemens D5000 powder X-ray diffractometer. Diffraction patterns were recorded with Cu$K\alpha$ radiation in step-mode between 20° and 80° 2θ, using a step-size of 0.02° and 2 sec/step.

Surface area and pore properties. Surface area and pore size information were obtained from nitrogen adsorption/desorption isotherms at 77 K, using a Micromeritics ASAP 2000 analyzer. Prior to measurement, all samples were degassed to 0.1 Pa. Gels treated above 393 K were degassed at 473 K, while gels dried at 393 K were degassed at this temperature. BET areas were calculated assuming a cross-sectional area of 0.162 nm^2 for the nitrogen molecule. Assessments of microporosity were made from *t*-plot constructions, using the Harkins–Jura correlation (*12*) for t as a function of p/p_0. Parameters were fitted to a low-area, nonporous silica. In cases where micropores were present, the surface areas reported are those obtained from the slope of the *t*-plot. Mesopore size distributions were calculated using the Barrett, Joyner, and Halenda (BJH) method, assuming a cylindrical pore model (*13*).

Selective reduction of NO with NH_3. Catalyst testing for the selective catalytic reduction of NO with NH_3 was performed in a 6-mm OD quartz tube reactor with on-line analysis of reactant and product gases by a mass spectrometer. The reactor bed consisted of 0.1 g of 0.3–0.5 mm granules of the dried gels. The reactor setup and the analysis methods employed have been described in detail elsewhere (*14*). The simulated stack emission feed consisted of 900 ppm NO and NH_3, 18,000 ppm O_2, with argon being the carrier gas. Routine testing involved an integral test and a differential test. In the former, the product yields of N_2 and N_2O were studied by increasing catalyst temperature at a constant space velocity of ca. 24,000 GHSV. Differential testing was performed in the 320–520 K range while maintaining conversion at 20% or lower.

RESULTS

Structural Transformation of Gels

Figures 1–3 show the structural transformations occurring during heat treatment of the vanadia, vanadia–titania and vanadia–titania–silica gels as revealed by the thermoanalytical and XRD investigations. The DTA and TG curves which were performed under air atmosphere show in general the following phenomena: dehydration, removal and oxidation of organic residues, transformation of titania and/or vanadia into crystalline phases, and melting of vanadia. All gels show the evolution of physisorbed and weak, lattice-bound water starting already at 300 K. The DTA curve of the vanadia Gel (V Gel) (Fig. 1) shows the crystallization of the vanadia (exothermicity with peak at 574 K) followed by its melting (endothermicity with peak at 949 K). XRD patterns (Fig. 1 bottom) of the sample before (sample corresponding to position A on DTA curve) and after (position B) the exo peak clearly indicate the crystallization. The loss of the weight (11.7%) (TG curve, Fig. 1) in the temperature range 300–570 K is due to the evolution of water and CO_2. Mass spectroscopic analysis of the evolved species showed a maximum in the water evolution rate at about 395 K, whereas CO_2 evolution became significant at about 430 K and reached a maximum at 530 K. The evolution of CO_2 is attributed to the oxidation of the isopropoxy groups remaining in the amorphous gel. Similar measurements carried out under an argon atmosphere (not presented) indicated that the vanadia contains V_3O_7 and V_2O_5 after crystallization (peak at ~600 K) and CO_2 evolution. The TG curve indicated that about 50% of the vanadia was reduced to V_3O_7 during crystallization, where the oxidation of the isopropoxy groups and consequently the CO_2 production was most prominent. Under air atmosphere (Fig. 1), the vanadia reduced is immediately re-oxidized (note small increase

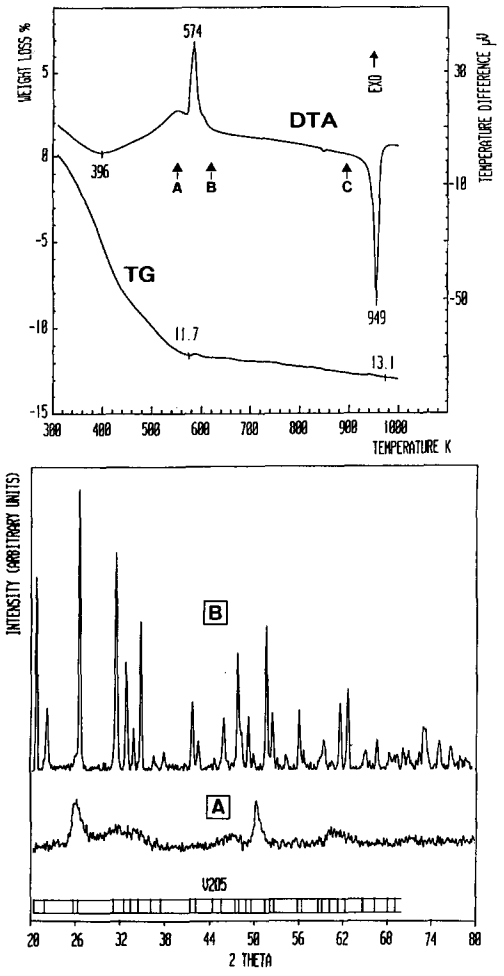

FIG. 1. Thermoanalytical (DTA and TG) curves and XRD patterns of vanadia gel heated under air. Heating rate 10 K min^{-1}; sample weight 20.2 mg; air flow rate 60 $cm^3 min^{-1}$. Temperatures at which samples were taken for XRD analysis are marked on DTA curve. XRD patterns of V_2O_5 calculated from JCDPS file 9-387 are shown as reference at the bottom of the figure.

of the weight on TG curve at about 580 K), and only well crystalline V_2O_5 is detected after the crystallization peak (samples B and C).

The DTA curve of the vanadia–titania gel (VTi Gel) (Fig. 2) measured under air atmosphere shows the following characteristic features. An endothermal peak due to the evolution of water appears at about 410 K, which is followed by exothermal peaks at 576, 676, and 737 K, and an endothermal peak at 947 K. Simultaneous mass spectrometric analysis of the evolved species showed the production of CO_2 during the first exothermal event (peak at 576 K), indicating the oxidation of organic residues of the precursor remaining in the gel. It is noteworthy to mention that sample B was still completely X-ray amorphous after this oxidation process. The exothermal peak at 676 K is due to the formation of small crystalline anatase domains, as was revealed by

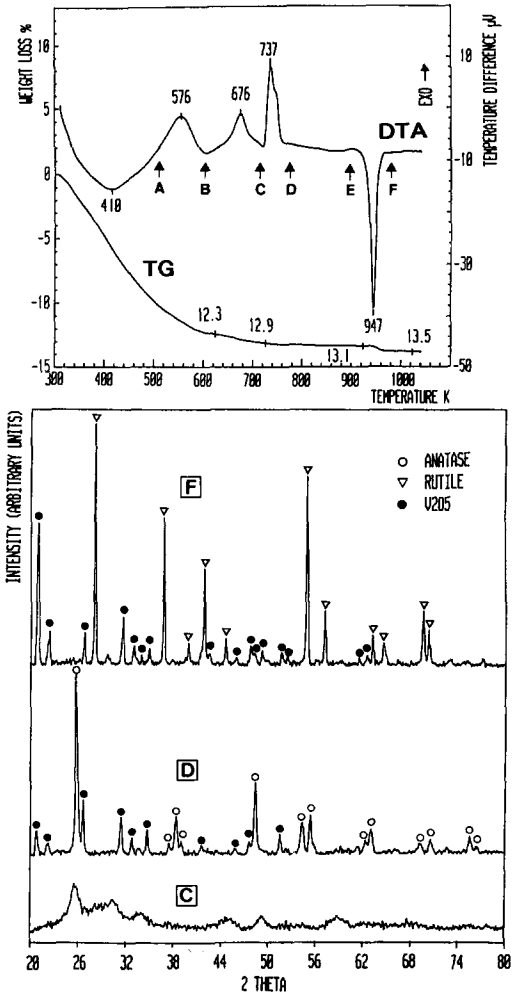

FIG. 2. Thermoanalytical curves and XRD patterns of vanadia–titania gel heated under air. Heating rate 10 K min^{-1}; sample weight 34.3 mg; air flow rate 60 $cm^3 min^{-1}$.

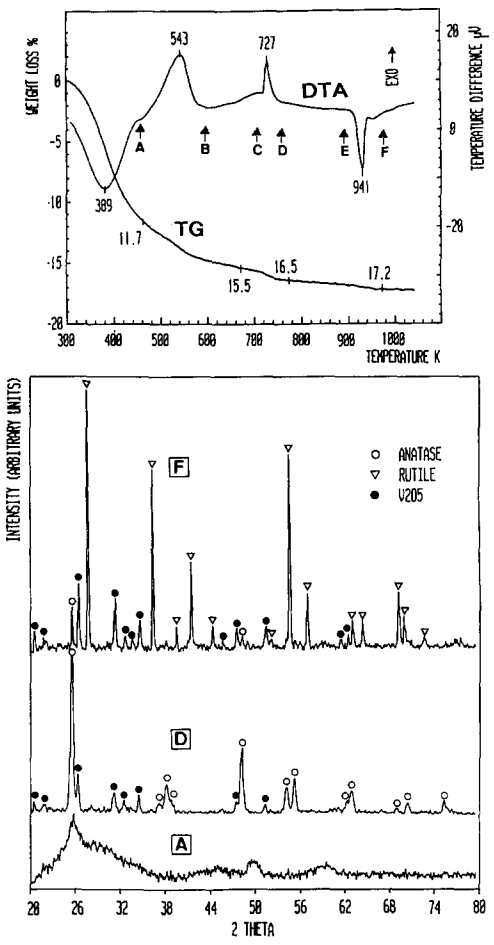

FIG. 3. Thermoanalytical curves and XRD patterns of VTiSi gel heated under air. Heating rate 10 K min^{-1}; sample weight 50.1 mg; air flow rate 60 cm^3min^{-1}.

XRD (trace C in Fig. 2) and TEM. The crystallization of V_2O_5 occurs at higher temperature (peak at 737 K with shoulder). This is confirmed by the XRD patterns of samples C and D shown in Fig. 2. Note that concomitantly with the crystallization of vanadia the crystallinity of anatase increases (compare trace C and D). Upon further heating to 900 K, the structure of the mixed oxide does not change significantly, as evidenced by XRD; however, after the endo peak (947 K) due to the melting of vanadia, the anatase has completely transformed to rutile (trace F). It seems likely that the melting and concomitant spreading of the vanadia phase accelerated the rutilization, since in measurements performed under similar conditions with pure titania complete rutilization was observed at significantly higher temperatures ($T > 1120$ K, (*15*)).

The major structural changes of the ternary vanadia–titania–silica gel (VTiSi Gel) occurring during heating in air are shown in Fig. 3. The first endothermal peak (389 K) in the DTA curve is again due to the removal of water, and the subsequent exothermal peak (543 K) to the oxidation of the organic residues orginating from remaining precursor materials, as evidenced by mass spectroscopy. In contrast to the ViTi Gel, with the ternary VTiSi Gel, the anatase and V_2O_5 crystallizations are not separate events, and there is no significant crystallization occurring with samples heated to ~700 K, as

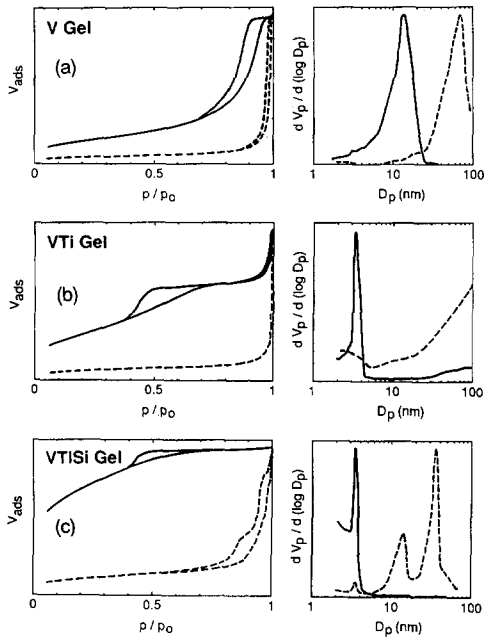

FIG. 4. Nitrogen adsorption and desorption isotherms of V, VTi, and VTiSi gels. Note that all *in situ* stabilized catalysts were exposed for 3 h to the reactant mixture flow at the given temperatures. (a) V gel, (——) 393 K, dried overnight; (– – –) 513 K, stabilized *in situ*. (b) VTi gel, (——) 513 K, stabilized *in situ;* (– – –) 870 K, stabilized in 7% O_2/Ar for 3 h. (c) VTiSi gel, (——) 513 K, stabilized *in situ;* (– – –) 870 K, stabilized in 7% O_2/Ar for 3 h.

TABLE 1

Textural Properties of Gel Catalysts Treated (Stabilized) at Different Temperatures

Conditions of pretreatment	Catalyst	V	VTi	VTiSi
393 K; dried overnight	SA (m^2/g)	94	—	—
	V^{tot}_{pore} (cc/g)	0.43	—	—
	V_{micro} (cc/g)	0.007	—	—
513 K; stabilized *in situ*, 3 h	SA (m^2/g)	27	139	340
	V^{tot}_{pore} (cc/g)	0.21	0.16	0.25
	V_{micro} (cc/g)	0.003	0.000	0.030
870 K, stabilized in 7% O_2/Ar, 3 h	SA (m^2/g)	—	11	53
	V^{tot}_{pore} (cc/g)	—	0.04	0.21
	V_{micro} (cc/g)	—	(0)	0.003

Note. SA represents BET surface area; V^{tot}_{pore}, total specific pore volume; and, V_{micro}, specific micro pore volume. V = vanadia gel, VTi = vanadia–titania gel, VTiSi = vanadia–titania–silica gel.

evidenced by XRD. Crystallization occurs with a maximum in the DTA curve at 727 K, and after this event the sample contains crystalline V_2O_5 and anatase only. Note that in contrast to the behavior of the VTi Gel there is no crystallization of anatase detectable by XRD below 700 K. Again the rutilization occurs mainly during the melting of the vanadia phase (endo peak at 941 K). After this event, rutile is the dominant phase, but some anatase is still present (cf. XRD patterns of sample F).

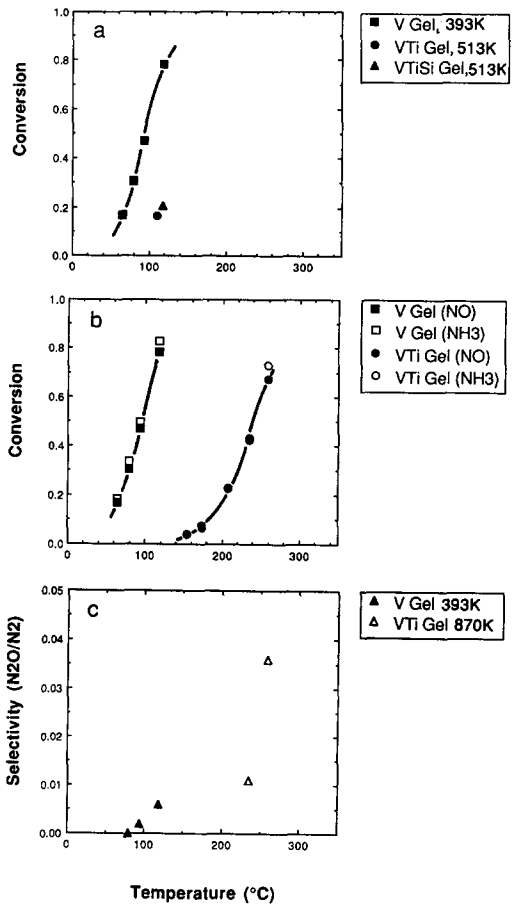

FIG. 5. Plots of conversion and selectivity for the reduction of NO with NH_3. (a) NO conversion vs temperature for amorphous gels. GHSV = 24,000–30,000 h^{-1}. (b) NO and NH_3 conversions for catalysts V gel (393 K) and VTi gel (870 K) GHSV = 24,000 h^{-1}. (c) Selectivity for N_2O as a function of temperature for V gel (393 K) and VTiSi gel (870 K).

TABLE 2

Apparent Activation Energies for the Selective Reduction of NO with NH_3 over Various Gel-Type Catalysts

Catalyst, treatment (temp, atmosphere)		E_{app} (kJ/mol)
V Gel,	393 K, *in situ*	48 ± 9[a]
	513 K, *in situ*	41 ± 9
VTi Gel,	513 K, *in situ*	49 ± 3
	870 K, in 7% O_2	57 ± 6
VTiSi Gel,	513 K, *in situ*	39 ± 2
	870 K, in 7% O_2	46 ± 7

Note. All *in situ* stabilized catalysts were exposed for 3 h to the reactant mixture flow at the given temperatures prior to commencement of the kinetic measurements.

[a] 95% confidence limits of estimated apparent activation energies.

Similar measurements carried out under argon atmosphere showed no distinct crystallization in the temperature range below 800 K. XRD analysis of samples taken after heating to 900 K indicated that these samples contained mainly rutile besides small amounts of anatase and traces of an unidentified phase which did not correspond to any pure vanadium or titanium oxide. After further heating to 1050 K (i.e., above the melt-

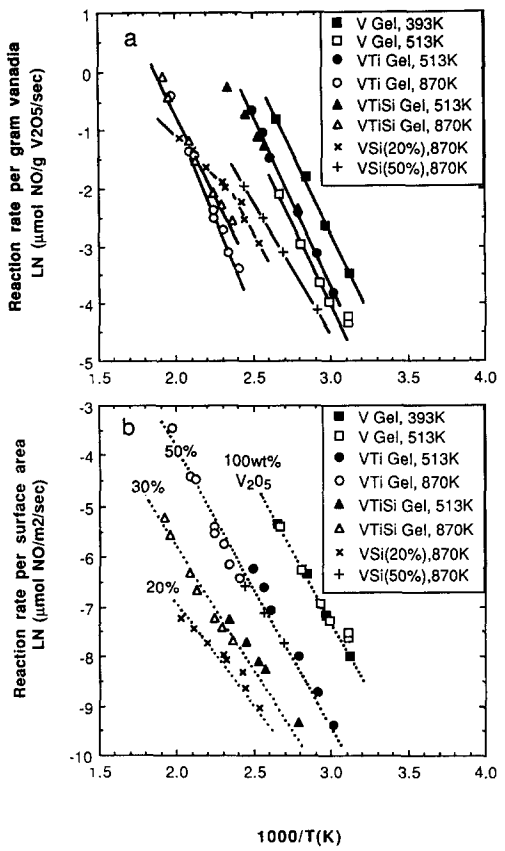

FIG. 6. Temperature dependency of NO conversion rate: (a) rate expressed per gram vanadia; (b) rate expressed per surface area of catalyst. Data for vanadia–silica mixed gels from Ref. (*9*).

ing temperature of V_2O_5) the reflections of the unidentified phase disappeared, and XRD indicated that the sample contained mainly rutile, little anatase, and traces of crystalline V_2O_5.

Surface Area and Pore Properties

The adsorption–desorption isotherms of the three gel materials are depicted in Figs. 4a–c and surface and pore volume data are listed in Table 1. All low temperature stabilized amorphous gels exhibit H2 hysteresis (IUPAC designation, (*16*)), indicative of mesopores with poorly defined size and shape. In low pressure regions, the knee in the adsorption isotherms of V(393 K) and VTi(513 K) Gels is well defined, whereas with VTiSi(513 K) Gel, the knee is more rounded, suggestive of Type I behavior in the filling of very narrow slit pores or micropores. The isotherm resembles more closely that of the pure component silica gel, rather than the vanadia–titania component, as represented by VTi(513 K) Gel. The distributions of mesopore diameters are unimodal and nearly symmetrical. The average pore diameters ($\langle d \rangle = 4V/A$) are 16 nm, 4.6 nm, and 2.5 nm for V(393 K), VTi(513 K), and VTiSi(513 K), respectively. The V and VTi amorphous gels are essentially non-microporous. In the amorphous VTiSi Gel, microporosity accounts for ca. 15% of the total pore volume (Table 1), though it has the

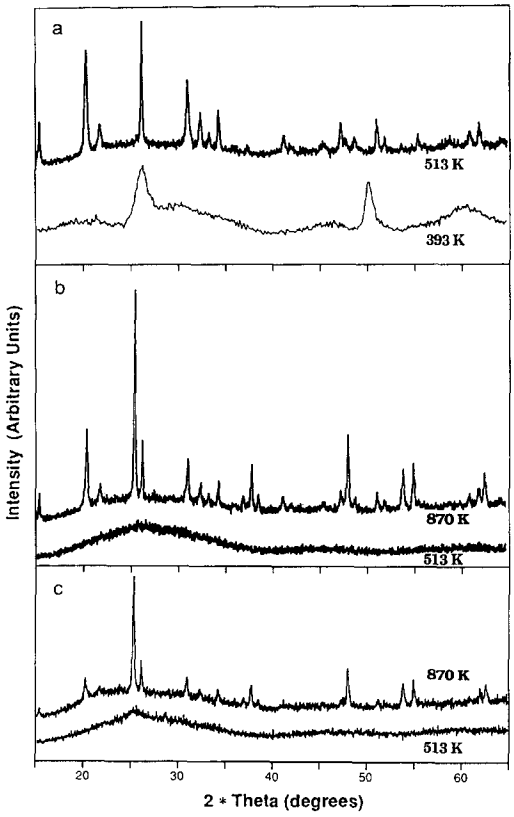

FIG. 7. X-ray powder diffraction patterns of gels after use in SCR experiments: (a) V gel, (b) VTi gel, (c) VTiSi gel. Temperatures indicated correspond to pretreatment (stabilization) temperatures.

highest mesopore area of the three gels, at 340 m^2/g contained in the 2.5 nm pores.

Surface area and pore properties undergo large changes at higher temperatures with the appearance of crystallization events. The pure vanadia gel is least stable, with crystallization of V_2O_5 after prolonged treatment at 513 K producing a shift of the hysteresis to high reduced pressure and Type H1 behavior. This type of hysteresis is associated with void spaces between globular particulates such as bulk crystallites. The shift in the pore diameter distribution to greater size and decreased pore volume also is indicative of general sintering behavior. Of the two 870 K treated gels, the VTi Gel experiences a one order of magnitude drop in surface area, and increase in pore size. The knee of the isotherm is sharper than before, since most of the micropores have disappeared. The mesopore development is more complex than the simple pattern established in the V and VTi Gels. Most of the 3–4 nm mesopores have been replaced by new pores of 11 nm and 25 nm sizes, the latter being the most predominant. Despite the sevenfold drop in mesopore area, the mesopore volume decline is only ca. 20% of the initial value. Pure component silica gel, treated at 870 K, contains only the small 3–4 nm mesopores, and in view of the sintering behavior of V and VTi Gels and phase separation into V_2O_5 and TiO_2 domains, these pores may represent regions of purely silica nature in the ternary gel, of which the silica content is 26% by weight.

Selective Reduction of NO with NH_3

All catalysts were stabilized under the reaction mixture flow for at least three hours at the temperature given in Table 2, prior to commencement of the routine testing procedure. Results from the integral tests show trends similar to those observed with other vanadia–titania catalysts (*17*). Figures 5a–c. depict typical conversion and selectivity relationships over the temperature range investigated. Ammonia conversion was up to 5% higher than NO conversion at higher temperature, due to a small loss to direct oxidation, but the primary reaction is represented by

$$NO + NH_3 + \tfrac{1}{4}O_2 \rightarrow N_2 + \tfrac{3}{2}H_2O.$$

As shown by the catalysts in Figs. 5b,c, N_2O production was minimal, with the highest levels, of several ppm, seen in catalysts tested near the upper temperature region. It should be noted that these levels are close to the detection limit of the analytical system. The amorphous V Gel displayed the highest NO conversion per bed volume of all gels, reaching 50% conversion (GHSV = 24,000), at 363 K (Fig. 5a). Data points obtained for VTi and VTiSi Gels in the amorphous state show similar conversion per bed volume, though at a 30 K higher temperature than for V Gel.

The temperature dependence of activity, expressed in terms of the NO conversion rate per weight of V_2O_5, is shown for all three gel preparations in Fig. 6a. The apparent activation energies (Table 2) are comparable to those of vanadia catalysts in dilute gas conditions and an oxidative environment (*1*). Of the amorphous catalysts, pure vanadia gel shows slightly higher activity than the mixed gel catalysts. More significant changes in activity occurred with crystallization of the vanadia component. The approximately threefold decline in activity per gram V_2O_5 of the V Gel, when thermally stabilized at 513 K, is not severe enough to decrease its turnover efficiency much below the one of the amorphous mixed oxide gels. A far greater decline is noted for the VTi and VTiSi Gels, calcined in 7% O_2/Ar for 3 h at 870 K before SCR testing. That these

FIG. 8. Transmission electron micrographs of various gel structures: (a) V gel (393 K), close-up shows fine structure; (b) V gel (513 K), platelet crystallites of V_2O_5; (c) VTi gel (870 K), two platelet V_2O_5 crystallites surrounded by small spherical anatase crystallites.

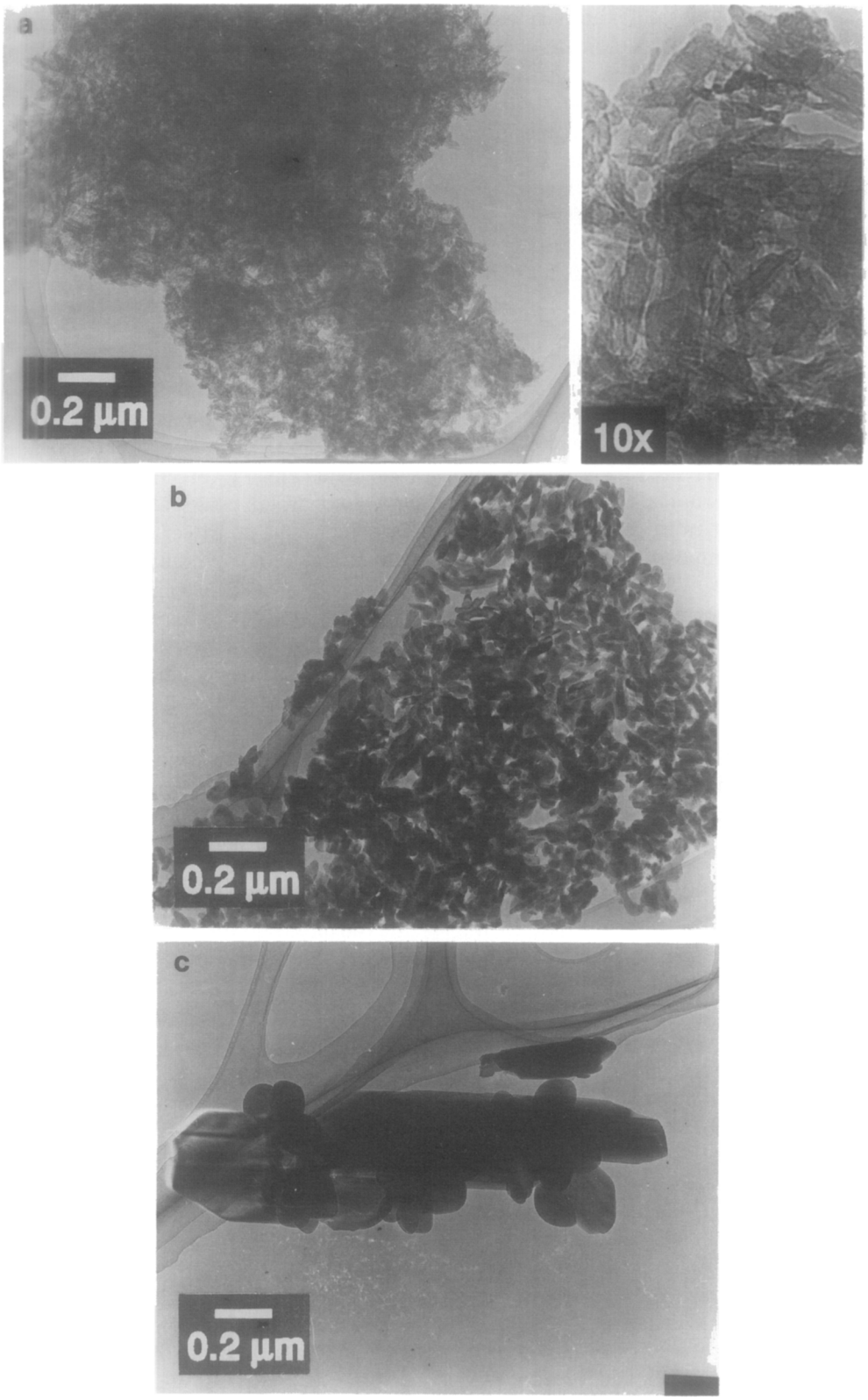
a
0.2 µm
10x
b
0.2 µm
c
0.2 µm

two catalysts display similar activity behavior (per V_2O_5) seems to indicate that the number of vanadia sites accessible for reaction is the same. It is interesting to note that the BET areas of the 870 K treated mixed gels differ by a factor of six. The BET area is non-selective (i.e., surface vanadia sites are not selectively titrated), yet if it may be assumed that the active site is not influenced by compositional or chemical effects, then the vanadia has achieved the same state of dispersion in both gels.

The correlation between activity decline and loss of dispersion is illustrated in Fig. 6b, where activity is expressed in terms of moles NO converted per unit area of surface, using the BET area for computation. Despite reductions in the BET area, the activity per catalyst area remains the same within each gel composition, the activity order being V Gel > VTi Gel > VTiSi Gel. The excellent correspondence between amorphous and crystalline catalysts of the pure vanadia gel clearly demonstrates the relationship between activity decline and loss of dispersion. Assuming that all components are homogeneously dispersed throughout the multi-component gels, the activity per surface area should vary with the vanadia content. This pattern is seen in the ordering according to gel composition, from the gel containing the least amount of vanadia (VTiSi) being least active to the pure vanadia gel being most active. However, the activity decrease with decreasing vanadia content is lower than expected from a simple component mixture. For instance, between pure and mixed gels, almost a twofold decrease would be expected for VTi (56 wt% vanadia) and nearly a threefold decrease for VTiSi (31 wt% vanadia). The actual activity decreases are by a factor of 6 and of 30, respectively. These discrepancies indicate that the vanadia dispersion in the mixed gel preparations is less than expected from a simple linear combination of pure components. An alternative explanation could be that a portion of the vanadia component is physically blocked or rendered chemically inactive by the mixing process. The relative vanadia area may be unchanged during the transformations in the mixed gels, and hence the amorphous and crystalline gel data superimpose on each other. Without more specific knowledge of the vanadia exposure, however, it is difficult to elaborate on other processes that might be involved.

XRD and TEM Analysis of Used Catalysts

Following the activity measurements, the morphology and crystallinity of all three gels were studied by transmission electron microscopy and X-ray powder diffraction. X-ray data (Fig. 7a.) of 393 K treated V Gel show two broad peaks at 26° and 50° 2θ, characterizing a poorly crystalline material. TEM analysis showed only weakly diffracting particles, even at high magnifications (Fig. 8a.), and selected area diffraction patterns did not show anything other than a diffuse ring, corresponding to the broad XRD peak centered at $2\theta = 26°$. The vanadia structures consisted of loosely interconnected sheets of varying sizes. Crystallization of bulk V_2O_5 is evident upon treatment of 513 K. The micrograph of the 513 K treated V gel (Fig. 8b.) shows that much of the very fine detail seen in 393 K treated gel is lost.

In the multi-component VTi and VTiSi Gels, crystallization into V_2O_5 and the anatase form of TiO_2 has taken place. Rutile was not detected. The V_2O_5 that appears in 513 K treated V gel, and in 870 K treated VTi and VTiSi Gels, exists in the form of highly crystalline platelets. Selected area diffraction patterns also confirm the presence of anatase crystallites. The micrograph of 870 K treated VTi Gel (Fig. 8c.) shows a well-developed V_2O_5 platelet surrounded by spherically shaped particles. Energy dispersive X-ray (EDX) and microdiffraction analysis of both particle structures showed that the spherical particles are pure anatase, and the platelets are made up of pure V_2O_5, with the (010) face exposed as the basal plane.

Within EDX detection limits, no vanadium emission was detected with anatase particles, nor was any titanium detected on the platelets; i.e., the vanadia and titania components are associated with separate structures. Although the silica matrix lowered electron beam transmission, the anatase and V_2O_5 morphologies in the 870 K treated VTiSi Gel are identical to those seen with the VTi gel. This is further supported by the XRD patterns shown in Figs. 2 and 3 (curves D).

DISCUSSION

Polymeric gels have been formed from vanadia oxo–hydroxo precursors via oxolation reactions, which form chains composed of $[VO(OH)_3(OH_2)]_n$ octahedral subunits, and by further reaction lead to a fibrous structure. Flat ribbons ~10 nm in length and 1 nm thick have been observed (*18*), and these are similar to the fibrous fine structure observed here. The poorly defined morphology lends itself to loose packing configurations that give it mesoporous structure. Vanadia dispersion could not be directly measured in the mixed gels. A rough estimate of the vanadia dispersion in the pure vanadia xerogel can be calculated using an assumed vanadia surface density of 4.9 V^{5+} sites/nm^2, from the (010) face of V_2O_5 (*19*), and the BET area. This yields a value of 0.8 mmol/g, or just under 10% dispersion. Yet it seems unlikely that the vanadia would be physically less dispersed than in pure xerogel form. Both pure component titania and silica sol produce xerogels of high area and mesoporosity, and this is evident in the mixed gel data. Crystallization into V_2O_5 platelets causes the decline of vanadia dispersion in all gels.

The thermoanalytical data (DTA) show the relative stability of the three gels, and are consistent with the surface area and pore results of gel samples subjected to prolonged exposure of low temperature SCR conditions. The pure vanadia gel is least stable of the three, and in order to maintain the high surface area of the amorphous structure it must be operated under SCR conditions not far above 400 K. Otherwise, a considerable loss in activity must be expected, due to the decline of surface area with crystallization.

The VTi Gel, however, provides a more stable amorphous structure up to 513 K. Treatment at higher temperatures under air eventually produced crystallization into spheres of anatase and platelets of V_2O_5. It is surprising that no evidence is found for a dispersed vanadia phase on the anatase crystallites, which usually forms during the thermal treatment of vanadia salt-impregnated TiO_2 catalysts.

In the amorphous VTiSi Gel, the vanadia component also exists in a highly dispersed state. This gel has the highest surface area, owing to its large silica component, and the highest resistance to dispersion loss by crystallization. As with the VTi Gel, bulk V_2O_5 and anatase phase coexist, but do not seem to be interacting. In spite of the silica matrix, the crystallization of vanadia in this gel does not seem to be sufficiently retarded in the 870 K treated (7% O_2/Ar) gel relative to the VTi Gel treated under the same conditions, and hence the vanadia dispersion is lost.

It is interesting to compare the activity of amorphous VTi Gel with that of a vanadia–silica mixed gel of 50 wt% V_2O_5 content reported previously (*9*). The V–Si gel (BET area, 94 m^2/g) was calcined in air at 870 K and characterized by high resolution electron microscopy and XRD as having ca. 20% of the vanadia in the form of microcrystalline (<50 nm), partially reduced bulk phases (V_3O_7, V_6O_{13}), but no crystalline V_2O_5 phase. This appears to demonstrate that the silica gel is more capable of retarding the crystallization and sintering of vanadia than the titania sol used in VTi Gel. Any retarding effect was absent, however, in the ternary VTiSi Gel investigated here.

On the activity per gram vanadia basis, better performance is seen with respect to the 870 K stabilized VTi or VTiSi Gels, yet poorer than these gels in their amorphous state. When compared on a per-surface-area

basis, the vanadia–silica gel activity line superimposes on the lines of the VTi Gel in both amorphous (513 K stabilized) and crystalline (870 K stabilized) state, implying that a similar state of vanadia dispersion has been reached in gel material of the same composition.

CONCLUSIONS

In summary, highly active, amorphous mixed gels containing vanadia can be prepared by the sol–gel method, exhibiting catalytic behavior for the SCR reaction similar to that of conventional, titania-supported vanadia catalysts. A loss in activity occurs upon thermal stabilization at elevated temperatures, due to surface area loss because of crystallization and particle sintering. Under the preparation conditions used in this study, the mixed gels were more stable to surface area loss than pure vanadia gel, with overall surface area best maintained in the silica-containing ternary gel. In spite of this, the addition of silica sol did not lead to a more efficient utilization of vanadia species for reaction; i.e., vanadia dispersion was not improved over the VTi gel, of lesser surface area but higher vanadia content.

ACKNOWLEDGMENTS

The authors acknowledge the assistance of R. Wessicken (Festkörperphysik, ETH-Hönggerberg) with analytical electron microscopy. This research was supported by grants of the Kommission zur Förderung der Wissenschaftlichen Forschung (Project 1774.1) and the Swiss Federal Institute of Technology.

REFERENCES

1. Bosch, H., and Janssen, F., *Catal. Today* **2,** 1 (1987).
2. U.S. Patent 4,789,533, December 6, 1988.
3. German Patent 2,458,888, May 23, 1979.
4. Haas, P. A., *Chem. Eng. Prog.* (April 1989).
5. Roy, R., *Science* **238,** 1664 (1987).
6. Mackenzie, J., *J. Non-Cryst. Solids* **100,** 162 (1988).
7. Ulrich, D., *J. Non-Cryst. Solids* **100**(1–3), 174 (1988).
8. Pearson, I. M., Ryu, H., Wong, W. C., and Nobe, K., *Ind. Eng. Chem. Prod. Res. Dev.* **22,** 381 (1983).
9. Baiker, A., Dollenmeier, P., Glinski, M., Reller, A., and Sharma, V. K., *J. Catal.* **111,** 273 (1988).
10. Baiker, A., Dollenmeier, P., Glinski, M., and Reller, A., *Appl. Catal.* **35,** 365 (1987).
11. Gasser, D., and Baiker, A., *J. Catal.* **113,** 325 (1988).
12. Carrott, P. J. M., and Sing, K. S. W., *in* "Characterization of Porous Solids" (K. K. Unger *et al.*, Eds.), p. 77. Elsevier, Amsterdam, 1988.
13. Barrett, E. P., Joyner, L. G., and Halenda, P. P., *J. Am. Chem. Soc.* **73,** 373 (1951).
14. Curry-Hyde, E., and Baiker, A., *Ind. Eng. Chem. Res.* **29,** 1985 (1990).
15. Handy, B., Gorzkowska, I., Nickl, J., Baiker, A., Schraml-Marth, M., and Wokaun, A., submitted for publication.
16. Sing, K. S. W., Everett, D. H., Haul, R. A. W., Moscou, L., Pierotti, R. A., Rouquerol, J., and Siemieniewska, T., *Pure Appl. Chem.* **75**(4), 603 (1985).
17. Baiker, A., Dollenmeier, P., Glinski, M., and Reller, A., *Appl. Catal.*, **35,** 351 (1987).
18. Legendre, L. L., and Livage, J., *J. Colloid Interface Sci.* **94,** 75 (1983).
19. Bond, G. C., Zurita, J. P., Flamerz, S., Gellings, P. J., Bosch, H., Van Ommen, J. G., and Kip, B. J., *Appl. Catal.* **22,** 361 (1986).